The International Journal of Fracture Mechanics, Vol. 4, Nr. 2, June 1968.
Wolters–Noordhoff Publishing – Groningen
Printed in the Netherlands.

LOCAL CRITERIA FOR DUCTILE FRACTURE

Frank A. McClintock

(Massachusetts Institute of Technology, Department of Mechanical Engineering, Cambridge, Massachusetts, U.S.A.)

ABSTRACT

Strain distributions in specimens suitable for studying the initiation of fracture are reviewed, and distributions are developed for the steady–state propagation of cracks in plane strain tension of fully plastic materials. The functional forms of local fracture criteria are discussed for different metallurgical mechanisms. It is concluded that:

a) pure Mode I (normal) fracture is unlikely to exist except in cleavage.

b) there is both theoretical and experimental evidence for the development of both sharp and flat–bottomed cracks.

c) simultaneous diffuse and concentrated (Dugdale–Muskhelishvili) flow fields can occur in torsion of longitudinally grooved bars if the stress–strain curve has a maximum which causes band formation, so that a displacement criterion becomes appropriate for final fracture.

INTRODUCTION

As in studying deformation, so in studying fracture it is easiest to focus attention first on a few idealized kinds of stress–strain behavior, such as linear elasticity, linear viscosity, non–hardening plasticity, rubber elasticity, and linear viscoelasticity. Interpolation between these idealizations gives insight into intermediate forms of behavior. Since the fracture of linear elastic materials is well understood as far as mechanics is concerned, this discussion will be focused on rigid–plastic, non–strainhardening materials as the next most important idealized mode of behavior in structural materials. Such behavior occurs not only in parts with overall plastic deformation, but also in very small regions at the tips of cracks in predominantly elastic structures. Simply for brevity, rate effects arising from stress–corrosion will not be considered, although there is no essential reason why they cannot be incorporated into a theory of fracture for ideally plastic materials.

The usual equations of continuum mechanics are by themselves insufficient to provide a fracture criterion because fracture is by definition the separation of a material into two parts at lower loads or extension than expected from continuum mechanics. Secondly, even the variables of stress and strain are sometimes insufficient for a fracture criterion because the continuum equations give stress and strain distributions that are identical for all sizes of geometrically similar specimens subject to similar stress or deformation boundary conditions, whereas for sufficiently large specimens of a geometrically similar class the nominal applied stress for fracture varies inversely as the square root of crack length. Finally, Rice[1] showed that the strain singularity at the tip of a sharp crack, particularly in torsion where there is no blunting, is of order $1/r$ to $1/\sqrt{r}$,

depending on the strain hardening. Such a singularity leads to an infinite strain (and stress, if the strain hardening is not saturated). Thus fracture would occur at once, if at all. Since this is not the case, some physical quantity in addition to stress and strain must play a role. In brittle fracture in tension, surface energy may be regarded as the needed quantity, but in compression Griffith[2] found it necessary to consider the maximum *local* strain energy (determined by local stress) on a crack similar in shape to those giving fracture in tension. Orowan[3] showed that the criterion for any state of stress could be interpreted as requiring the ideal cohesive strength near the tip of a crack whose tip radius was of the order of atomic dimensions. Thus a linear dimension can provide the needed physical quantity in addition to stress and strain.

Any criteria for ductile fracture must take into account the fact that a number of processes or stages are involved, whose relative importance differs from one material or configuration to another. For instance, holes or microcracks may be nucleated by dislocation interactions, the fracture of inclusions, or the separation of inclusions from the matrix. The resulting holes can grow by plastic flow, local fracture along grain boundaries, sliding off, or hole growth on an even smaller scale. The growth of the holes may be accelerated by the localization of the applied deformation into thin bands either as a result of strain softening or mechanical instability due to the growth of the holes themselves. Holes growing in such bands not only elongate but also rotate, tending to overlap. The cracks may be stable or unstable even in the relatively rigid grips of a testing machine. Clearly a variety of fracture criteria will be required to characterize these different stages. To illustrate some of the variables involved in a criterion, we shall first consider the growth of holes, which is the archetype of ductile fracture. After expressing the criterion for brittle fracture in a similar fashion, we shall consider other important parts of the ductile fracture process with intermediate forms of fracture criteria.

IDEALIZED FRACTURE CRITERIA

Criteria for initial yielding or for brittle fracture require only the current state of stress. In ductile fracture by the growth of holes, however, the changes in size, shape, and spacing of the holes depend on the entire history of stress, strain, and rotation, because in plastic flow the current stress determines only the current increment of deformation, with most of the current configuration being determined by prior deformation. To simplify a representation of the strain history, consider for the moment only cases in which the principal components of applied stress do not rotate relative to the material, although they may vary in magnitude. In other words, consider the normal fracture and the delamination types of fracture shown in Fig. 1, but not the shear fracture. Only the principal components of stress and strain need then be considered. Assuming the holes to be relatively small over most of the life of the specimen, the components of applied stress and strain (on a scale large compared with the spacing between the holes) will be related by the usual stress–strain relations for an incompressible, rigid–plastic material, giving just three independent variables. The most symmetrical representation is in terms of the three normal strain deviators (only two are independent) and the mean normal stress $\underline{\sigma}$. Since the sum of the normal strain deviators is zero, the strain can be represented in triangular coordinates on a single plane. Such a coordinate system is shown in Fig. 2, along with the final shapes of an initially cubic element deformed along various radial paths. The cartesian coordinates of the specimen are labeled $\underline{a}$, $\underline{b}$, and $\underline{z}$ to correspond to major, minor and axial directions of elliptical holes to be discussed below.

For any increment in principal strain, the corresponding components of stress can be determined from the stress–strain relations. The components of strain increment and stress in turn

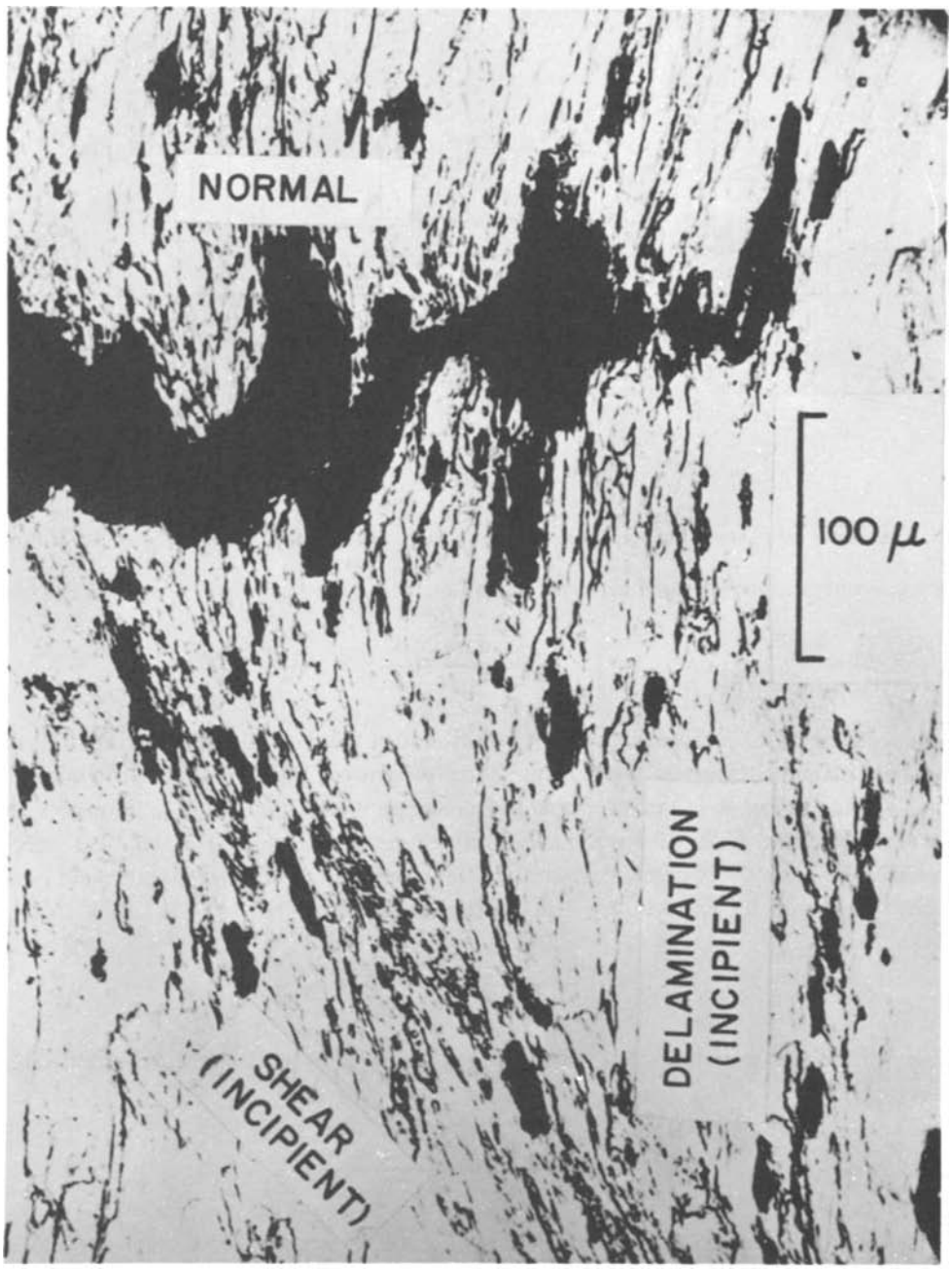

Fig. 1. Growing normal fracture and incipient delaminating and shear fractures in necked copper tensile specimen. Bluhm and Morrissey (1965). Courtesy of U.S. Army Materials Research Agency.

determine the relative growth and coalescence of holes, leading to fracture. McClintock[4] has developed an approximate fracture criterion based on the assumption of cylindrical holes parallel to the z axis, subject to generalized plane strain. If the holes have an elliptical axis $2b$ and a spacing ℓ_b in the b direction, then the damage associated with their coalescing in the b direction

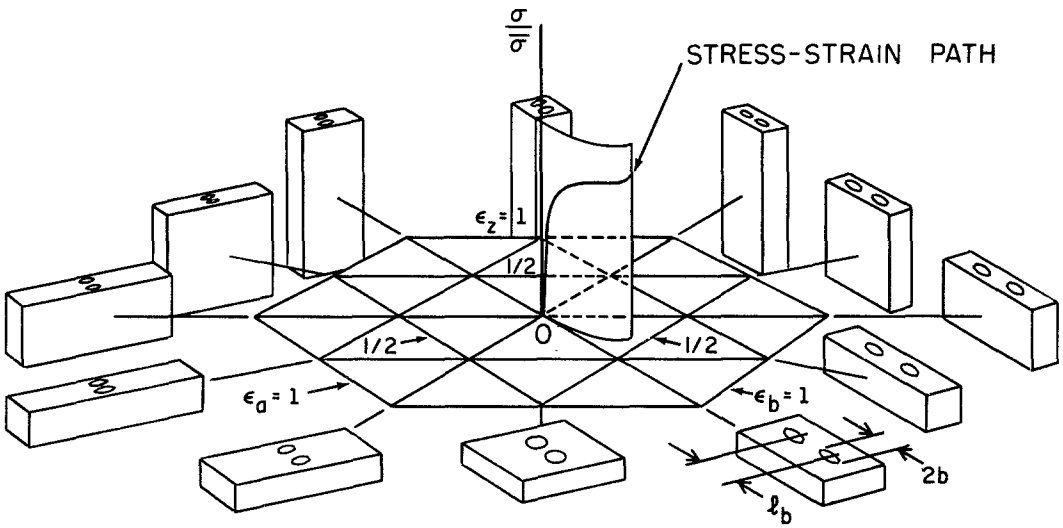

Fig. 2. Strain plane with corresponding deformations of a cube containing z holes coalescing in the b direction.

may be given in terms of a required relative growth factor F_{zb} by

$$d\eta_{zb} = \frac{d\,\ell n(2b/\ell)}{\ell n\, F_{zb}}. \tag{1}$$

Since at coalescence the damage is taken to be unity, and at that time 2b is equal to ℓ_b, the growth factor is approximately given in terms of the initial dimensions by $F_{zb} = \ell_b^o/2b^o$. Berg's[5] solution for viscous materials was extrapolated by comparing it with the plastic solution to yield an equation for elliptical holes with applied transverse stress components σ_a^∞ and σ_b^∞. The effects of strain hardening were approximated in terms of the exponent n in $\bar{\sigma} = \sigma_1 \bar{\epsilon}^n$, where $\bar{\sigma}$ and $\bar{\epsilon}$ are the equivalent stress and strain respectively. The damage rate is approximately

$$\frac{d\eta_{zb}}{d\bar{\epsilon}^\infty} = \frac{\sinh\,[(1-n)\,(\sigma_a^\infty + \sigma_b^\infty)/(2\bar{\sigma}/\sqrt{3})]}{(1-n)\,\ell n\, F_{zb}} \tag{2}$$

In general this rate must be integrated along a path in Fig. 2; in particular for constant ratios of stress components,

$$(\bar{\epsilon}^\infty)^\rho = \frac{(1-n)\,\ell n\, F_{zb}}{\sinh\,[(1-n)\,(\sigma_a^\infty + \sigma_b^\infty)/(2\bar{\sigma}/\sqrt{3})]}. \tag{3}$$

This locus is plotted in Fig. 3. The physical quantity besides stress and strain that seems essential to a fracture criterion very likely arises from the fact that the critical strain must be attained over an element of material containing at least a few holes. For instance, if inclusions serve as the nuclei for the holes, the length dimension would be the inclusion spacing.

If the holes are relatively large, the assumption of incompressibility is no longer valid. Instead, the mean normal stress is limited by the yield condition of the material and the third variable becomes the volumetric strain. The choice of the coordinates of Fig. 2 is also useful for describing the stress–strain history of a part subjected to low cycle fatigue, especially if the path is not a plane figure corresponding to fixed ratios of strain components. The fracture locus for brittle

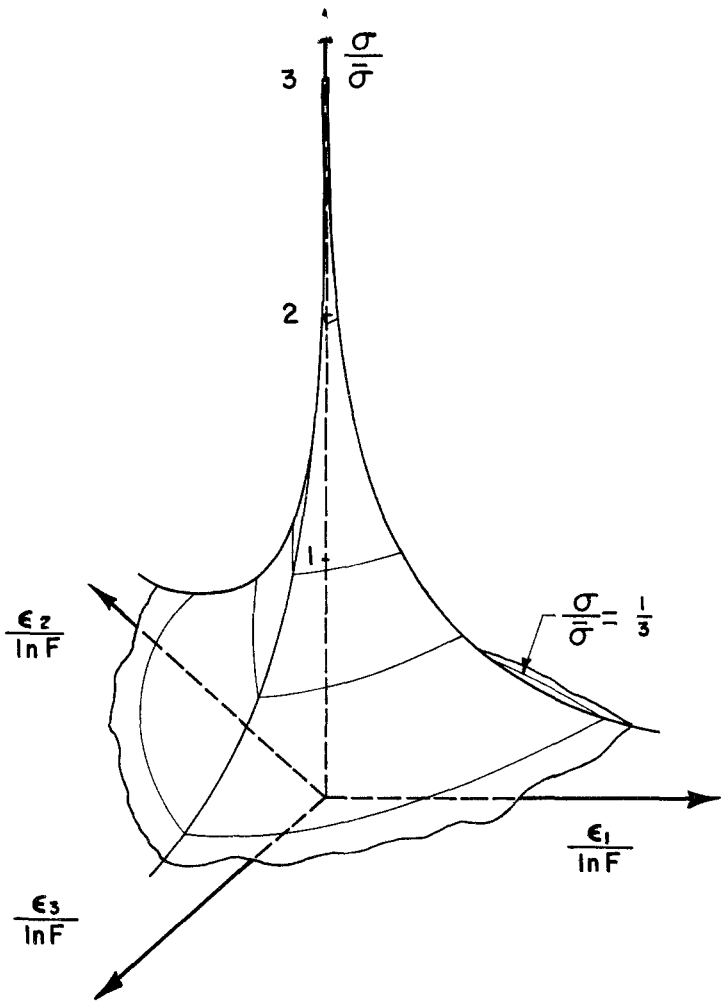

Fig. 3. Ductile fracture locus for irrotational flow with constant stress ratios.

material under combined stress can be expressed in similar terms, using deviatoric strain and mean normal stress, as shown in Fig. 4.

CRITERIA FOR CRACK INITIATION

A. Stress and Strain Distributions.

In order to study the initiation of fracture experimentally, it is necessary to have specimens with controlled states of stress, especially triaxiality, in regions in which the strain distribution is known. Close to the crack tip the plastic parts of the strain are large compared with the elastic in most metals and alloys. Fully plastic specimens may then be used to determine ductile fracture criteria, especially since elastic–plastic distributions are still not well understood near the crack tip. In brittle materials, of course, the plasticity may be too limited to make the fully plastic theory appropriate. The critical question is whether the extent of the plastic zone is large compared with the structure of the material. The extent is estimated from the critical stress intensity factor K_c and the flow strength Y by

$$R_c = (1/\pi)\,(K_c/Y)^2 = (k_c/Y)^2 = (\sigma_\infty\sqrt{c}/Y)^2 \tag{4}$$

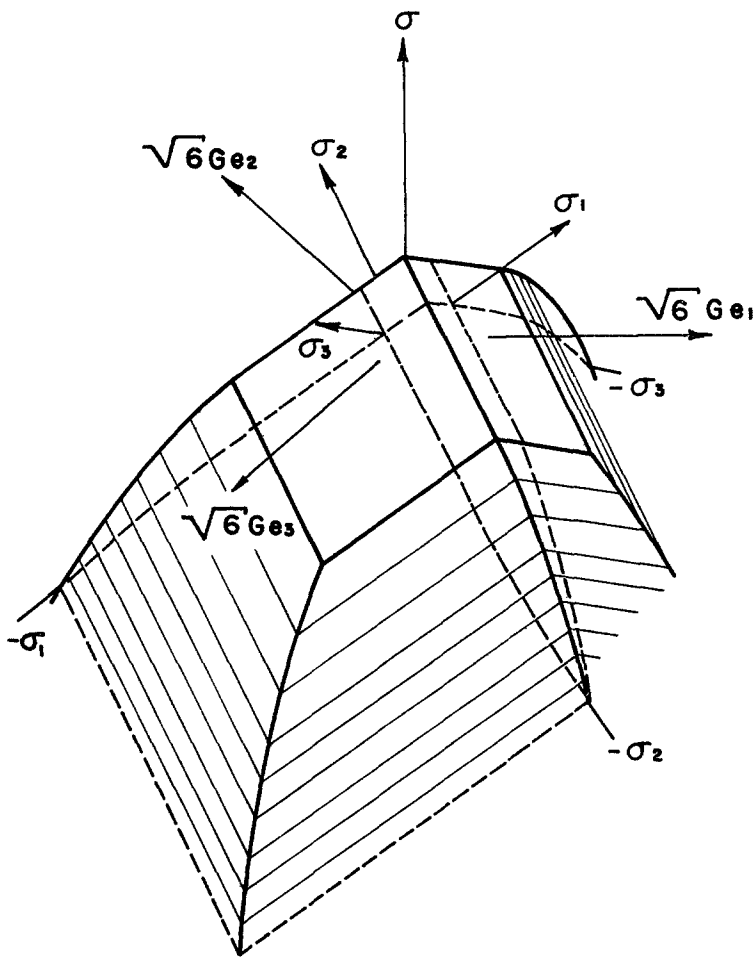

Fig. 4. Griffith fracture locus in terms of strain deviators.

The fully plastic *stress* distributions in plane strain of a non–strainhardening material have been known for some time. The principles and a number of examples are given by Hill[6] and Prager and Hodge[7]. A summary of the literature, giving the limit loads and required shoulder thickness, was given by McClintock[8]. See also Hundy[9].

1. For a *doubly–grooved, plane strain specimen in tension,* the strain distributions were found by Neimark[10] who used the uniqueness theorem of Hill[11] for slightly strain hardening materials to show that the strain in the flank and in the diamond–shaped region of the doubly grooved specimen of Fig. 5 should be uniform, but that in the fans above and below the tip of the crack the strain varies approximately as $1/r$. Such specimens, if designed to study the initiation of fracture under high triaxial stress, must meet several criteria:

a) They must fracture in the diamond–shaped core rather than at the root of the groove. Therefore the ratio of strain in the root to that in the core must be less than the ratio of the fracture strains at the two different triaxialities. While this ratio could be estimated from Eq. 3, that estimate would be too high because Eq. 3 overestimates the ductility at low triaxiality. With our present fragmentary experimental data (Edelson and Baldwin[12]; Alpaugh[13]; Hodges[14])

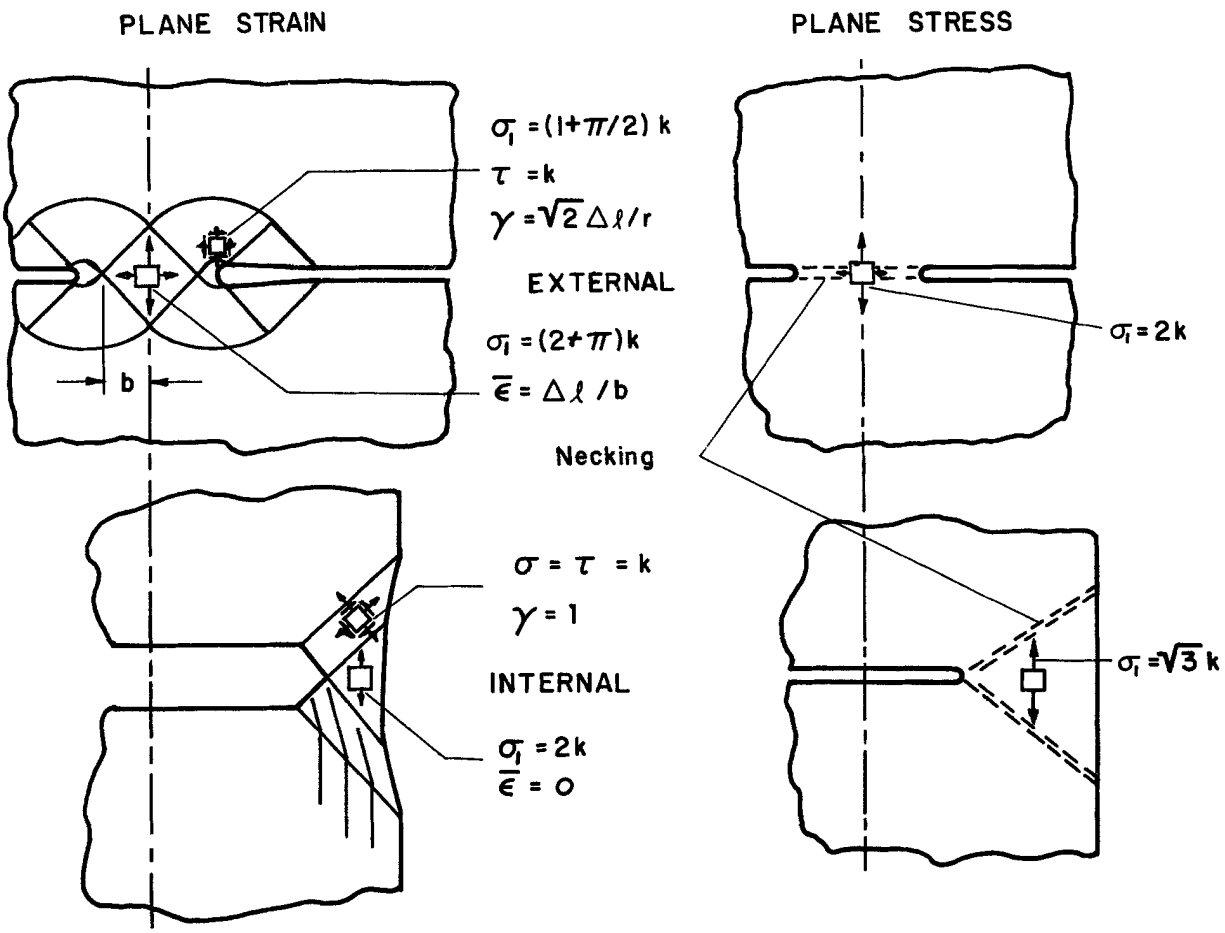

Fig. 5. Fully plastic flow fields in tension.

it seems reasonable to take as a limit, in terms of the included flank angle ω:

$$\frac{\epsilon_{root}}{\epsilon_{core}} < 1 + (5 \text{ to } 15)\,(1 - \omega/\pi), \tag{5}$$

where the numerical coefficient tends to be low for highly strain–hardening materials and conversely. The strain ratio is found from the results of Wang[15], along with Neimark's result[10], that the core strain per unit displacement up and down from the center section is

$$\epsilon_{core} = u/b, \tag{6}$$

where in turn the core half–width b is found from the equation for the extent of the logarithmic spiral subtending the root of a groove with included angle ω and root radius ρ_g:

$$a - b = \rho_g\,[e^{(\pi-\omega)/2} - 1]. \tag{7}$$

Values of $\epsilon_{root}/\epsilon_{core}$ are plotted in Fig. 6 as a function of a/ρ_g for various values of the included flank angle ω.

b) The specimen must not fracture at the tip of the logarithmic spiral before cracking in the

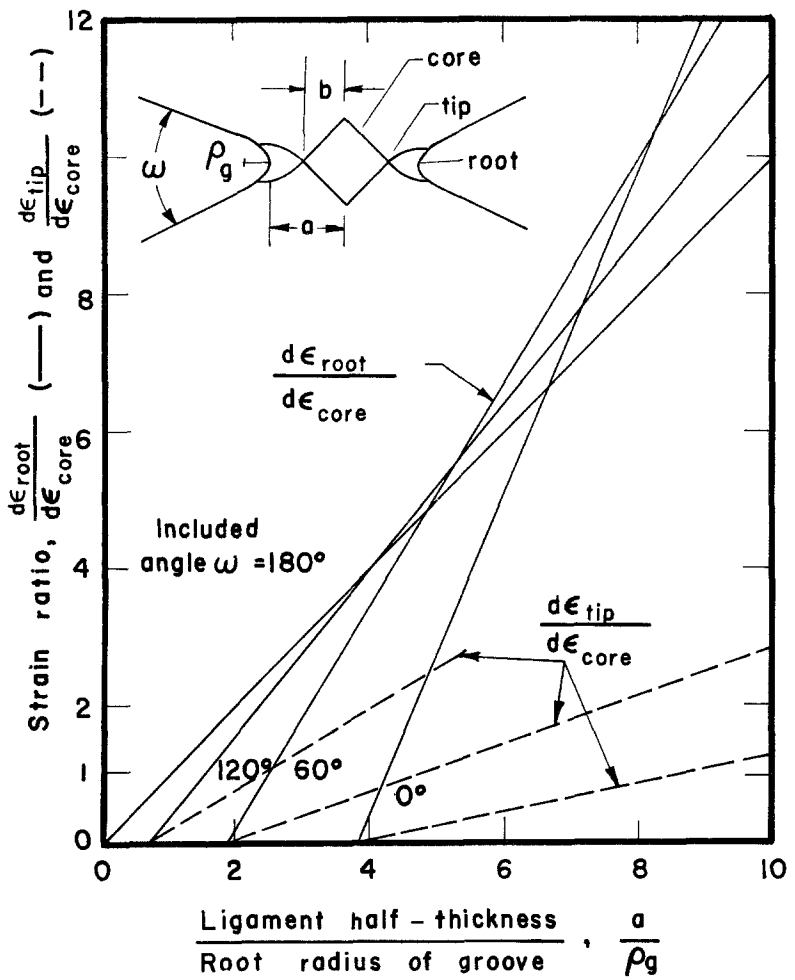

Fig. 6. Required shoulder width for full triaxiality in doubly grooved, plane strain tensile specimens.

core. The strain there, found from Wang[15] is plotted in Fig. 6 as dashed lines:

$$\frac{d\epsilon_{tip}}{d\epsilon_{core}} = \frac{a/\rho_g + 1}{e^{(\pi-\omega)/2}} - 1. \tag{8}$$

c) The core region of high strain should be a large fraction of the ligament thickness so that its central region will be relatively unaffected by rounding–off of the strain distribution due to strain hardening, especially after the expected extension. This criterion may mean choosing the smallest root radius (largest ligament) satisfying criteria a) and b) above. For ductile materials it may be necessary to re–machine the groove at an intermediate stage in the test.

d) Once the proportion between root radius and ligament thickness has been chosen, the size must be made large enough so that a number of fracture nuclei, such as grain sizes or inclusion spacings, are included in the core section. More practically, the specimen must be large enough to machine, handle, and observe conveniently.

e) Next the shoulders must be chosen as large as shown in Fig. 7 (after Neimark[10]), so that yielding of the shoulders is prevented and the full triaxiality guaranteed. For very ductile materials that strain harden, the shoulder ratio should perhaps be further multiplied by the ratio

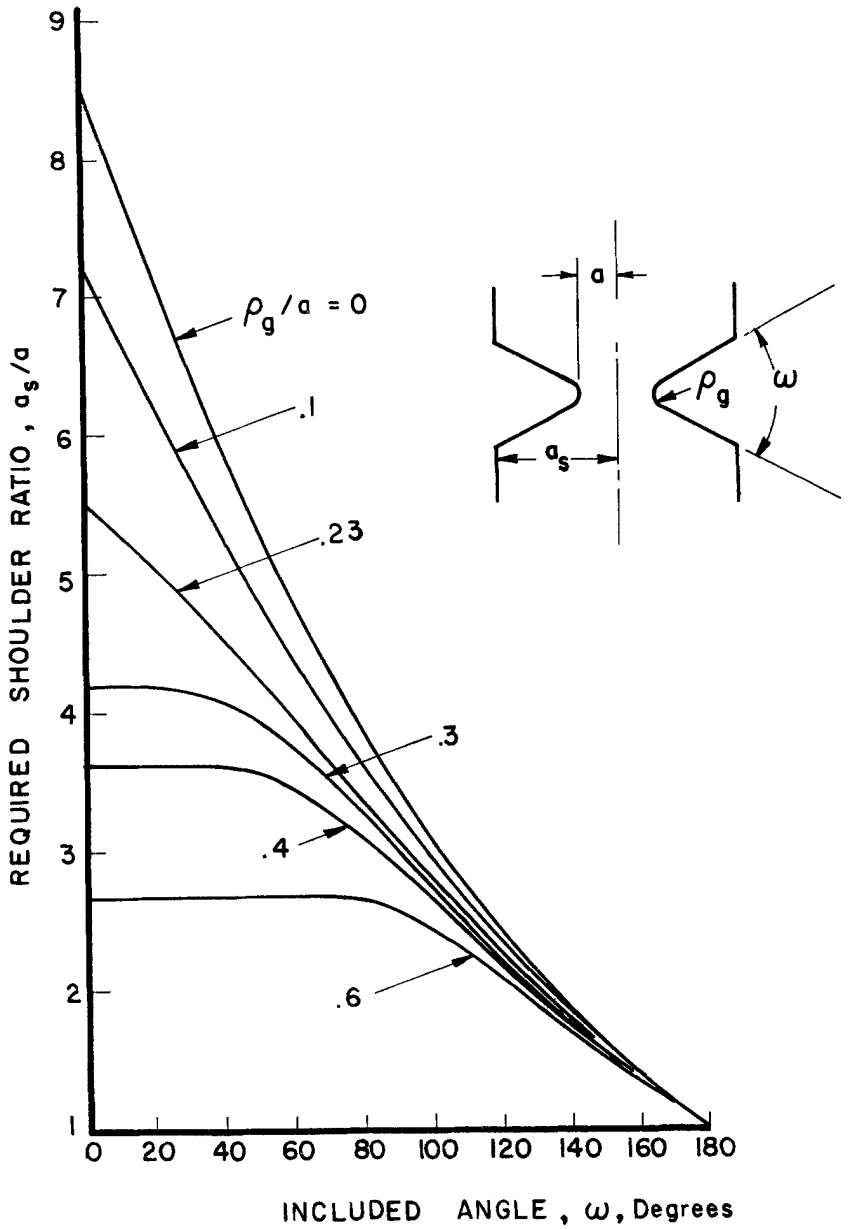

Fig. 7. Required shoulder width for full triaxiality in doubly grooved, plane strain tensile specimens.

of, say, (tensile / yield strength) $(2/\sqrt{3})$ to give some assurance that fracture will occur in the minimum section before yielding in the shoulders under uniaxial stress.

f) Finally the total width of the specimen (parallel to the grooves) should be chosen to be large enough so that plane strain is guaranteed at the center of the specimen. This probably requires a total width of specimen of twice the total shoulders thickness for $\omega = 0$ to $10a_s$ as $\omega \to \pi$, or as much as 20 times the ligament thickness. (See Findley and Drucker and also Ewing and Hill[16].

2. *Asymmetrically grooved, plane strain tensile specimens* may be of two types: opposing with unequal angles, which will be discussed later in connection with crack propagation, and anti–symmetrical grooves which enforce combined shear and rotation under various amounts of mean normal

stress, as discussed by Guillen–Preckler, et al.[17]. Further asymmetry, caused by making these grooves unequal or by staggering them, leads to combined Mode I and Mode II fracture. Such sections should be placed in mirror images along a specimen to allow lateral motion, and are best carried out in rigid rather than pivoted grips.

3. *For round tensile specimens,* Bridgman[18] showed that in naturally necked specimens the strain distribution was uniform across the section, and that this led to a triaxial stress at the center of the neck. Clausing[19] pointed out that this strain distribution does not hold for specimens with machined necks. Norris[20] has shown that the effect of a pre–machined neck depends on the rate of strain hardening. The approximate strain distributions obtained by Norris have not yet been integrated to give the stress history in the specimen.

4. *In plane stress* (thickness < R/10), a fully plastic non–hardening material necks immediately, as indicated in Fig. 5. An overall fracture criterion should be based on the extension across the neck, or on the reduction of area, as suggested by McClintock[21] and Rosenfield et al.[22] In more detail, a crack propagates across a sheet by 'shear' at 45° to the tensile direction and the plane of the sheet. Very close to the tip of the crack the deformation corresponds to combined Mode I and Mode III, with the three components of displacement depending on the two coordinates in the plane normal to the leading edge of the crack. This rather complex state has not been analyzed. With strain hardening, or neglecting thinning, the strain is diffuse, as analyzed for example by Swedlow et al.[23] or observed by Bateman, et al.[24].

5. In *torsion* Walsh and Mackenzie[25] compared the theoretical elastic–plastic strain in circumferentially grooved specimens of a non–hardening material with tests on 7075–T6 aluminum alloy. Similarly, Kayan[26] studied crack initiation in fully plastic, longitudinally grooved specimens.

So far, most of the analysis has been for specimens where initiation occurs in relatively uniform strain fields. It would be of interest to study the classes of possible local plastic strain fields that can exist around sharp notches before crack growth, as will be done below for crack propagation, to see what substitutes for the elastic stress intensity parameter K can be found in the plastic range. One example of such a result is the analysis by Rice[1] for effects of strain hardening in a groove loaded in Mode III. Fracture in such tests would be affected by size or strain gradient effects in a way not apparent from smooth specimens.

B. Modes of Crack Initiation.

TABLE I

Local Criteria for the Initiation of Fracture

A. On an atomic scale
1. Perfect lattice: $\sigma_1 = \sigma_2 = \sigma_3 = 0.02$ to 0.04 (bulk modulus B) over 10 Å.
2. Vacancy condensation: $\sigma_{crit} = 2$ (surface tension, γ)/r over 10r, with r radius of existing nucleus, or $\nu^1_{Debye} \exp(\gamma r^2/kT)$ is reasonable time. Then growth is a function of time.
3. Single dislocation: $\sigma_1 = \sigma_2 = \sigma_3 = \sigma = 0.01$ to 0.02B over ~ 10 (Burgers vector, b).
4. Dislocation arrays:
   a. Two opposing edge dislocations on parallel α planes: $f(\sigma_{\alpha\alpha}, \sigma_{\alpha\beta}, b/\ell)$ over dislocation spacing, ℓ.
   b. End of low angle boundary: $f(\sigma_{\alpha\alpha}, b/\ell)$ over ℓ.
   c. Dislocation tangle: $f(\sigma_{\alpha\alpha}, \sigma_{\alpha\beta}, b/\ell)$ over ℓ.
5. Grain boundary separation: $\sigma_1 = \sigma_2 = \sigma_3 = 0.01$ to 0.02B over 10 Å.

B. On a microscopic scale

6. Dislocation pile up: $f(\sigma_{\alpha\beta}-\sigma_{friction}, \sigma, \epsilon_{\alpha\beta}^{p})$ over dislocation path $\underline{d}$ (which is grain diameter, slip band spacing, or twin band spacing). Little relaxation by slip in other directions.
7. Twin band intersection: $f(\sigma_{\alpha\beta}, \epsilon_{\alpha\beta})$ over twin length.
8. Triple point: $f(\epsilon_{\alpha\beta}, \sigma)$ over grain boundary $\underline{d}$ (little adjacent relaxation).
9. Brittle phase cracking: $f(\sigma, Y(\bar{\epsilon}))$ over $\underline{d}$.
10. Inclusion separation: $f(\sigma, Y(\bar{\epsilon}))$ over $\underline{d}$.
11. Cleavage coalescence: $\sigma=\sigma_{crit}$ over several cleavage sites followed by $\sigma = f$(displacement).
12. Hole coalescence: $\int f(\sigma, n, d(rot.)/d\bar{\epsilon})d\bar{\epsilon} =$ critical value over inclusion spacing (See Eqs. 1 to 3, 9 to 11, for example.)
13. Mechanical instability: $f(\sigma_{max}, \bar{\epsilon}, n) = 0$ over hole spacing or sheet thickness.
14. Metallurgical instability: $f(\sigma_{max}, d\bar{\sigma}(\bar{\epsilon})/d\bar{\epsilon}) = 0$ over grain size or slip band length.

A number of modes of crack initiation are listed in Table 1, along with variables expected in criteria for fracture. Certain further comments are in order.

1. A *perfect lattice* requires equal triaxial stress for the initiation of fracture because the shear strength decreases as the dilatation increases[27].

2. *Vacancy coalescence* is possible at high temperature where the vacancy concentration is high. The expression here gives the critical stress for the applied stress to just offset the surface tension that tends to contract the hole, but neglects the decrease in free energy due to the disappearance of the vacancy that migrates into the hole. This energy is difficult to estimate, because as shown by Versnyder in Sullivan's[28] review of fracture, holes tend to form in those grain boundaries that are normal to the applied direction of stress, so the energy considered should be that of a vacancy in a grain boundary, so to speak, rather than in a crystal lattice.

3. *A single dislocation* in a close–packed, relatively ductile crystal again requires nearly pure hydrostatic tension for fracture. The strength is reduced below that for a perfect lattice by a factor of about 2, according to the bubble raft model, which appears to represent the behavior of a monovalent ductile metal better than any power function or exponential force law (McClintock and O'Day[27]. Fracture occurred by an opening up of holes rather than by cleavage, even though cleavage sometimes seems to be pending as the dislocations widen under increasing tension.

4. *Dislocation arrays* are of many kinds. *Two opposing edge dislocations* with the missing half plane between them can provide some of the tension needed to form a hole at another dislocation between them. The fracture criterion then involves not only the hydrostatic tension but also a shear stress component that helps to drive dislocations together. In most dramatic example of fracture being nucleated, Gilman[29] showed that in zinc crystals, in which the motion of one part of a *low angle grain boundary* produced cleavage on the basal plane in zinc. Here Stroh[30] has calculated an orientation dependence of tensile strength for zinc crystals that agrees well with the experimental results of Deruyttere and Greenough[31].

Under combined stress one would expect fracture to occur on some combination of normal stress and shear stress on the slip plane. More generally, of course, there are very intense *tangles of dislocations* for which no theory of fracture has been obtained.

5. *Grain boundary fracture* can occur either by separation of grain under purely hydrostatic tension[27] or by the motion of dislocations into the grain boundary from one crystal which cannot be accommodated by slip in the other.

Often times the initiation of fracture on an atomic scale does not lead to microscopic fracture because the nucleation sites are not sufficiently close together or because the initial cracks are

stable. In such cases a fracture criterion must be satisfied over a microscopic region of the order of a few grain diameters or inclusion spacings before fracture can be considered to occur from the continuum point of view. In other cases the complexity of the deformation process simply makes it easier to consider regions of several microns or several grain diameters in size. We now turn to such a microscopic point of view.

6. *Dislocation pile–ups* first bring in the amount of plastic strain, which may be small. With sufficiently long pile–ups the cracking is produced almost entirely by shear stress, and is nearly independent of normal stress. An example is shown in MgO by Johnston, Stokes, and Li[32].

7. *The intersections of twin bands* can also provide the stress concentrations necessary to produce local fracture (Hull[33]). Here again, the condition for fracture depends on the friction and twinning stresses in the material, the applied shear stress, and the normal stress in some complex way for which a criterion cannot yet be given.

8. *Holes at triple points or steps in grain boundaries* can result from grain boundary sliding, occurring at high temperatures. Thus grain boundary hole growth, as opposed to cleavage or inclusion cracking, usually appears only in creep.

9. *The cracking of brittle phases* has also been frequently observed metallographically, for example, by Cottrell[34]. A clear metallographic example obtained with replica techniques is shown in Fig. 8. Brinkerhoff[35] has shown that under longitudinal shear with rigid inclusions the shear

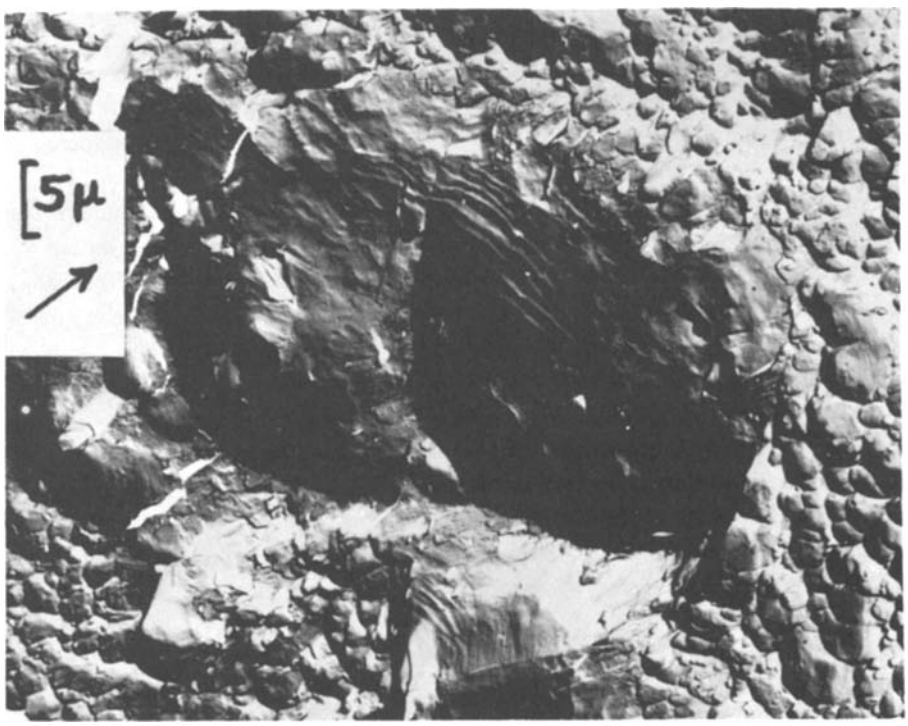

Fig. 8. Electron micrograph of a replica of fracture in 6061 aluminum alloy under combined tension and torsion, showing cleavage, sliding off, and hole growth. Crack growth and shadowing in direction of arrow. Courtesy of R.M.N. Pelloux.

strain around a rigid inclusion may reach infinity, but the stress within the inclusion is limited to perhaps twice the flow strength of the matrix. It seems reasonable to expect that similar results hold

for cylindrical or spherical inclusions, although the drag on long cylindrical inclusions aligned with the direction of maximum tensile strain may result in a normal stress within the inclusion of the order of the flow strength of the matrix times the length to diameter ratio of the inclusion, as discussed in studies of composites such as Kelly and Davies[36]. This leads to criteria in which fracture is controlled by the sum of the maximum principal stress applied to the material plus some factor times the yield or flow strength of the matrix.

10. *Inclusions may separate from their matrix* not only in the ellipsoidal manner reported by Palmer and Smith[37] but also, when rotation is involved, with rather sharp tails as shown by Tipnis and Cook[38].

11. *Cleavage coalescence* may be needed to initiate fracture because the cleavage of some grains will reduce the triaxiality in others so that the cleavage stops. Also cleavage planes in adjacent grains will rarely have a common intersection with the grain boundary. The remaining holes must be joined together by hole growth, discussed below. This intermittent fracture has been frequently observed, for example by Knott and Cottrell[39]. Some of the ductile fracture linking the cleavage facets is seen in the upper right portion of the scanning electron micrograph in Fig. 9. Thus, for the

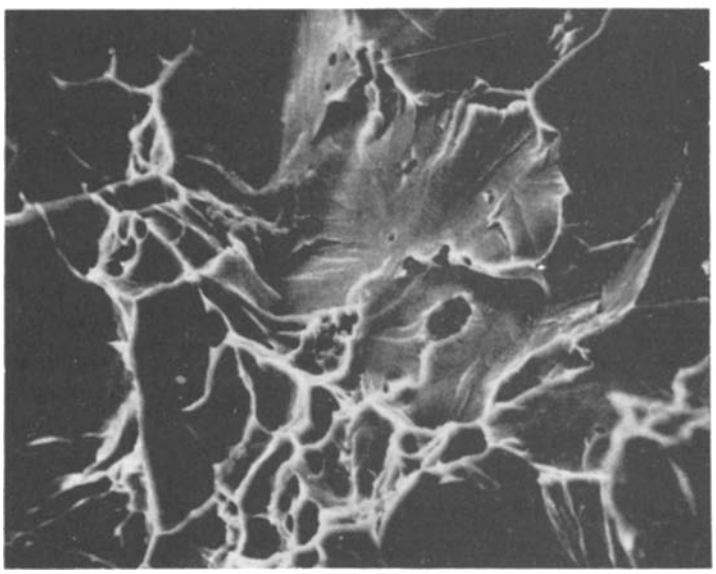

Fig. 9. Transition from hole growth to cleavage fracture in 1020 steel at room temperature. Scanning electron microscope at about 2000x. Courtesy of R.M.N. Pelloux.

first time, fracture is not so much a single abrupt event as it is a process. A stress criterion is needed to describe the initiation, after which the normal stress is a function of displacement during the plastic flow necessary to link up the cleavage planes in adjacent crystals.

12. *The plastic coalescence of holes* has been discussed above and is given in Table 1 for strain with no rotation, and by McClintock, Kaplan and Berg[40] for the coalescence of holes in shear bands. They found that holes of initial mean radius R_1, spaced a longitudinal distance L_L apart along the shear band, and subject to a shear strain γ, would exhibit a relative growth given by

$$\ell n\, F_L = \ell n(L_L/2R_1) = \ell n \sqrt{1+\gamma^2} + \ell n\, R/R_1 . \tag{9}$$

whereas for holes initially spaced a distance L_T apart in the thickness direction of the shear band to coalesce in that direction the required growth ratio was simply

$$\ell n\ F_T = \ell n(L_T/2R_1) = \ell n\ R/R_1. \tag{10}$$

In either case the growth in mean radius of the holes was governed by the shear stress τ in the band, the normal stress across it, σ, and the strain hardening coefficient in the expression $\tau = \tau_1 \gamma^n$ according to the equation

$$\ell n\ R/R_1 = \frac{\gamma}{2(1-n)} \sinh \frac{(1-n)\sigma}{\tau}. \tag{11}$$

13. *Mechanical instability* due to lack of any large amount of strain hardening seems to lead to the formation of shear bands that link up holes, as shown for example in Fig. 1. On a more quantitative scale Alpaugh[13] studied the effect of triaxiality on ductile fracture of mild steel, using specimens pre–necked by various amounts. He found fracture occurred at values of the relative hole growth ratio that were only a fraction of those expected from metallographic observation of the inclusion density. Postulating that the presence of the holes tended to produce a local shear band formation, McClintock[41] estimated the degree of strain hardening at which the mechanical instability would occur. In every case but one the actual fracture occurred even earlier, especially in the case of specimens of cold rolled steel, pre–necked with an initial ratio of cross–section radius to profile radius of 4, where the fracture strain dropped to 1/7th of that for a straight specimen. Fractographically the surfaces were still similar, so there is no reason to suspect a different mode of fracture. Further work is required in view of approximate nature of the analysis and the uncertainty of the stress and strain distribution associated with using the Bridgman analysis on such a pre–necked specimen (Norris[20]). The instability may also account for the relatively low ductilities observed by Edelson and Baldwin[12] compared with Eq. 3.

14. *Metallurgical instability* can occur in alloys as a result of over–aging or reversion (Forsyth, Stubbington, and Wilson[42]. An example is the shear bands observed both under monotonic loading and fatigue in 7075–T6 aluminum alloy (McClintock[43]; McClintock and Argon[44]). Such strain softening can lead to the concentration of shear so that very small applied displacements cause intense local strains and fracture from other causes. The effect is the same as that of mechanical instability without the necessity for changes in shape.

CRITERIA FOR CRACK GROWTH

A. Fully Plastic Stress and Strain Distributions

1. Introduction

As with initiation, many of the mechanisms of crack propagation require appreciable *plastic* strain, and may therefore be studied in appropriate fully plastic specimens. To see the parameters that might be used in fracture criteria, we first consider several fully plastic stress and strain distributions around propagating cracks. These distributions can differ from elastic ones in that 1) the strain depends on the past history, not solely on the currently applied stress, and 2) there are a variety of stress and strain states for Mode I deformation, even in plane strain. Nevertheless, the assumptions of the local nature of the fracture process and of steady state growth together limit the class of stress and strain distributions and histories that may be encountered. Perhaps, then, there are parameters, analogous to the stress intensity K of elasticity, that in combination serve to describe criteria for crack propagation. In this spirit, we ignore the detailed process of crack growth, whether by sliding off, hole growth, zig–zagging, or other mechanisms, and seek the stress and strain distributions in surrounding areas that are far enough away from the crack tip so that the material can

be regarded as a continuum, but close enough so that the rigid–plastic approximation is valid.

1. *Torsion of a circumferentially grooved bar* of non–hardening material results in rigid body rotation of all but the plane of minimum cross–section. The only variable with which to describe fracture is the relative displacement v across the discontinuity. Assume that the crack propagates past a point when

$$v = v_c. \tag{12}$$

The displacement per unit twist is equal to the radius:

$$\frac{dv}{d\phi} = r. \tag{13}$$

For ease in later generalization, consider the total displacement at r to be that acquired before crack growth plus that during crack growth from $\xi = 0$ to c:

$$v = v_c \frac{r}{r_0} + \int_0^c r \frac{d\phi}{d\xi} d\xi. \tag{14}$$

This equation can be integrated directly; the critical displacement $v = v_c$ is required when the crack reaches r:

$$v_c \left(1 - \frac{r}{r_0}\right) = r(\phi - \phi_c), \quad \text{or} \tag{15}$$

since $\phi_c = v_c/r_0$,

$$\phi = v_c/r = v_c/(r_0 - c). \tag{16}$$

This result could have been obtained directly, but the above formulation applies as well when the strain rate at a point depends on the current crack position, so that Eq. 14 becomes a non–trivial integral equation.

The solution of the integral equation by assuming $d\phi/dc$ constant can be easily checked here; it leads to

$$\frac{d\phi}{dc} = \frac{v_c(1-r/r_0)}{rc} = \frac{v_c}{r_0(r_0-c)}, \tag{17}$$

as opposed to the correct value,

$$\frac{d\phi}{dc} = \frac{v_c}{(r_0-c)^2}. \tag{18}$$

If, following the ideas of Barenblatt, the stress falls off, say, linearly to zero as the displacement is increased from v_c to v_f, direct integration gives the torque–twist curve of Fig. 10. Sectioning and metallographic examination at $\phi > w_f/r_0$ should reveal damage between $r = v_c/\phi$ and $r = v_f/\phi$. This mode is likely to be found only with strain softening materials; strain hardening would broaden the band, reduce the local displacement per unit twist ahead of the crack (i.e. reduce the first term of Eq. 14) and increase the twist per unit crack growth. Insight might be obtained from the solution for a viscous material, obtained by analogy from the elastic solution. For convenience, the limiting case of an infinitely deep notch could be used.

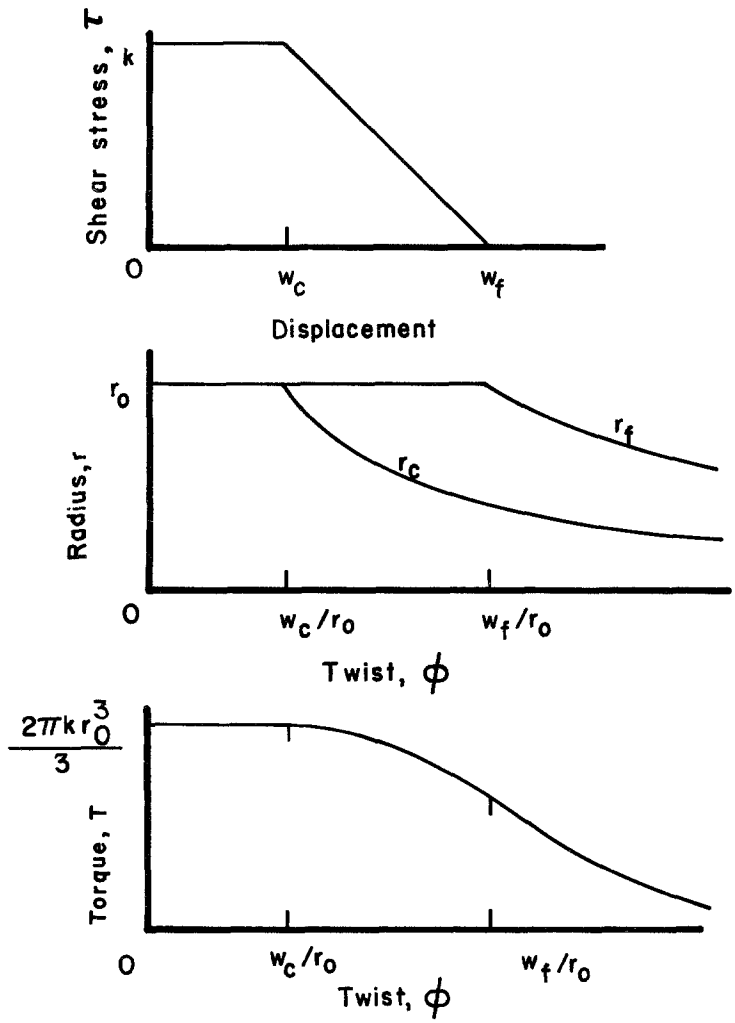

Fig. 10. Torque–twist of a circumferentially grooved bar in torsion with no strain hardening.

The circumferentially notched specimen illustrates what seems to be a general principle: that if plastic deformation is limited to a band and there are no rate effects *per se*, the loading on an element is monotonic with constant ratios of stress components (radial loading), so no history effects can appear in a fracture theory.

2. *Torsion of a longitudinally grooved bar* provides a simple example including history effects, and in which the fracture criterion may be either of the strain or displacement type. The cross–section shown in Fig. 11 allows a steady–state crack propagation rate. First consider the stress–strain curve (a) of Fig. 11 in which fracture is abrupt. At a given point x, y the strain increment is given in terms of the angle of twist per unit length ϕ and the radius R through that point from the crack tip to the residual elastic core. In terms of $\theta = \tan^{-1} y/(x-\xi)$,

$$d\gamma_{\theta z} = \left(\frac{R^2}{y/\sin\theta} - \frac{y}{\sin\theta} \right) d\phi. \tag{19}$$

The ratio of components of strain referred to axes fixed in a material element, $d\gamma_{xz}/d\gamma_{yz}$, changes as the crack progresses. Therefore, before integration of Eq. 19, it is necessary to ask what

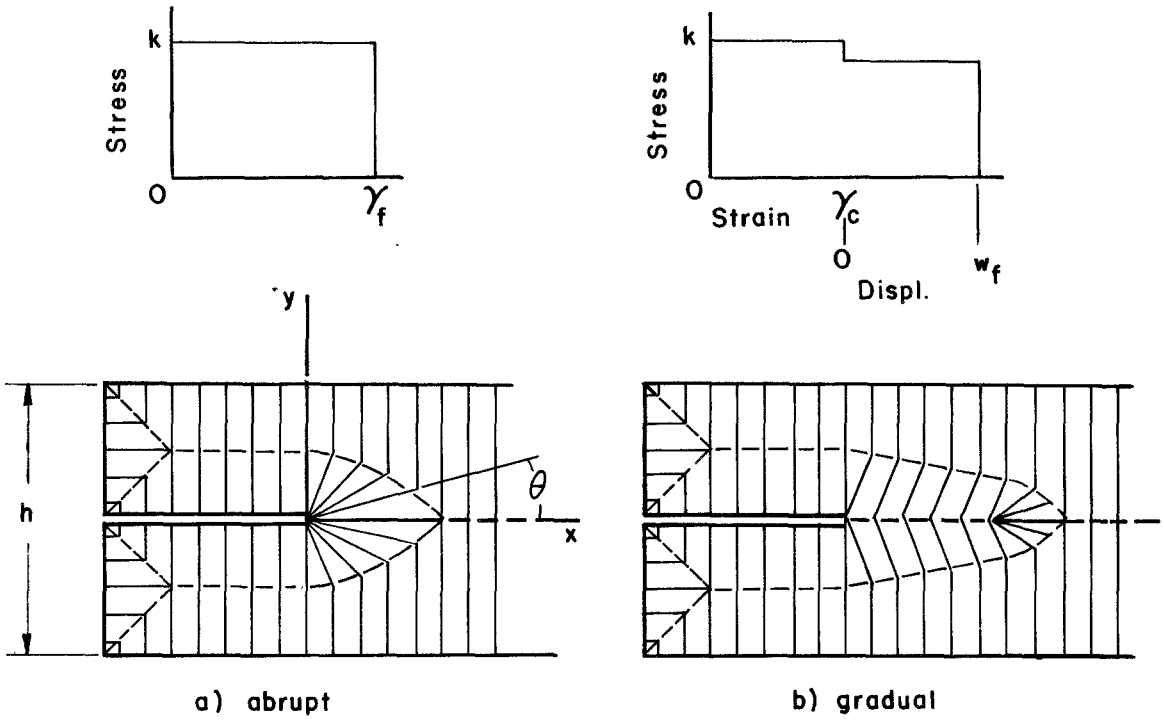

Fig. 11. Slip lines in a longitudinally grooved bar in torsion with abrupt and gradual fracture.

component of strain is critical for fracture – for example, accumulated equivalent strain, equivalent accumulated strain, displacement across some given element up to a given angle to the plane propagation, or strain accumulated on the planes of maximum strain. Since cracks are observed to grow almost directly ahead, it seems most reasonable to consider the strain at points close to the plane $y=0$ and within an angle ϕ of the crack direction. For example, take the strain component at an angle α to the x axis. Integrate from the crack coordinate when the plastic zone first reached the point, $\phi \approx y/(h/2)$, to $\phi \approx (30^\circ)$. The angle of twist is expressed as twist per unit crack growth, $d\phi/d\xi$. The change in crack coordinate is found from:

$$x-\xi = y/\tan\theta \quad \text{or} \quad d\xi = y\,d\theta/\sin^2\theta. \tag{20}$$

Finally, for a rectangular bar of thickness h,

$$R(1+\sin\theta) = h/2. \tag{21}$$

Combining Eqs. 19 through 21,

$$\gamma_{\alpha z} = \gamma_{\theta z}\cos(\theta-\alpha)$$
$$= \int_{y/(h/2)}^{\theta\approx 30^\circ} \cos(\theta-\alpha)\left[\frac{h^2}{4}\frac{1}{\sin\theta(1+\sin\theta)^2} - \frac{y^2}{\sin^3\theta}\right]\frac{d\phi}{d\xi}\,d\theta. \tag{22}$$

Since a steady state geometry exists, the crack growth rate may become constant. If so, $d\phi/d\xi$ can be factored out at its steady state value. In order to achieve a simple solution, keep only the largest terms, assuming θ, α, and $y/(h/2)$ are all small compared with unity:

$$\gamma = \frac{d\phi}{dc}\frac{h^2}{4}\,\ell n\left(\frac{h\theta}{2y}\right) = \frac{d\phi}{dc}\frac{h^2}{4}\,\ell n\left(\frac{h}{2x}\right) \quad \text{for} \quad \theta, x/h, y/x \ll 1. \tag{23}$$

Thus the equation given by McClintock[45] for the strain directly in front of the crack is valid also within angles of about ± 30° to either side.

It seems necessary to consider conditions in some region of finite size ahead of the crack. Otherwise, at the crack tip itself (x = 0), an infinitesimal angle of twist could cause infinite strain. If the fracture process is by repeated nucleation, the strain at a point one nucleation spacing in front of the crack will be critical; strictly, the integral of Eq. 22 should be replaced by the corresponding sum.

A criterion based on the displacement of one flank relative to the other includes strains over angles up to 90°, which would have little to do with the material that was fracturing and would be different for non–rectangular cross–sections, such as a circular one, where the strain is relatively much less for $\theta > 30°$. If the fracture is gradual and continuous, the strain field in front of the crack will be distorted by the 'softening' of the material. This softening will in turn lead to a band formation, which must then be described in terms of displacements across the band. The field of characteristics will be distorted as indicated in Fig. 11, where the warping displacements must give the amount of softening that corresponds to the stress discontinuity in the band. No analysis has yet been made.

3. Next consider *admissible fields for Mode I* (tensile) crack propagation. First, is the tip blunt or sharp? This question should be answered by the mechanics of the problem, but it is helpful to start with the right assumption. Experimental data indicate a sharp angle, of the order of 10°, in brass, steel, and aluminum alloys. In more ductile materials, such as aluminum and copper, angles of 60° to 90° were found, in accordance with Rogers[46] results on double cup fracture. The theory predicts 90° for a singly grooved specimen, in general agreement with Rogers' results. We therefore conclude that sharp cracks do occur, although not in all metals, for lead was an exception.

In formulating the general equations for Mode I, it turns out to be convenient to start with the strain distribution. To satisfy incompressibility, assume a stream function which is in general a function of $\underline{r}$ and $\underline{\theta}$. Postulate that for small $\underline{r}$ the stream function can be represented by a leading term consisting of a function of θ times powers of the radius and its logarithm:

$$\dot{\psi}(r, \theta) = F_{mn}(\theta)\,[r^n\,\ell n^m(r)]. \tag{24}$$

The corresponding displacement rates, or velocities, keeping only the largest terms for small $\underline{r}$, are

$$\begin{aligned} \dot{u}_r &= \frac{1}{r}\frac{\partial \psi}{\partial \theta} = F'_{mn}(\theta)\,[r^{n-1}\,\ell n^m(r)], \\ \dot{u}_\theta &= -\frac{\partial \psi}{\partial r} = -F_{mn}(\theta)\,[nr^{n-1}\,\ell n^m(r)]. \end{aligned} \tag{25}$$

The strain rates, again dropping all but the largest terms, are

$$\begin{aligned} \dot{\epsilon}_r &= \frac{\partial \dot{u}_r}{\partial r} = F'_{mn}(\theta)\,[(n-1)r^{n-2}\,\ell n^m(r)] = -\dot{\epsilon}_\theta \\ \dot{\gamma}_{r\theta} &= \frac{\partial \dot{u}_\theta}{\partial r} - \frac{\dot{u}_\theta}{r} + \frac{1}{r}\frac{\partial \dot{u}_r}{\partial \theta} \\ &= [-n(n-2)F_{mn}(\theta) + F''_{mn}(\theta)]\,r^{n-2}\,\ell n^m(r). \end{aligned} \tag{26}$$

The rotation may also be required:

$$\dot{\phi} = \frac{1}{2}\left[\frac{\partial \dot{u}_\theta}{\partial r} + \frac{\dot{u}_\theta}{r} - \frac{1}{r}\frac{\partial \dot{u}_r}{\partial \theta}\right]$$
$$= \frac{1}{2}\left[-n^2 F_{mn}(\theta) - F''_{mn}(\theta)\right] r^{n-2}\, \ell n^m(r). \tag{27}$$

For symmetrical flow, $F_{mn}(\theta)$ must be an even function of θ. For a crack with finite included angle ω, the circumferential velocity must be zero along the flank:

$$F_{mn}(\pi - \omega/2) = 0. \tag{28}$$

If there is rigid–body motion before and behind the crack, the radial velocity must be independent of r both for $\theta = 0$ and $\theta = \pi - \omega/2$. It is then necessary that $n = 1$ and $m = 0$. The only component of strain is then shear (taking care not to include terms that dropped out in an earlier differentiation):

$$\dot{\gamma}_{r\theta} = \frac{F_{01}(\theta) + F''_{01}(\theta)}{r}. \tag{29}$$

There is then only the corresponding component of stress. To determine the possibility of strain hardening, calculate the accumulated equivalent strain by integration along a streamline, where the time increment is expressed in terms of that required for an element to traverse an increment of angle:

$$\bar{\epsilon} = \int_{-\infty}^{t} \dot{\bar{\epsilon}}\, dt = \int_0^\theta \frac{\dot{\bar{\epsilon}}}{\dot{u}_\theta} r\, d\theta = \int_0^\theta \frac{\dot{\gamma}_{r\theta}}{\sqrt{3}\dot{u}_\theta} r\, d\theta$$
$$\bar{\epsilon} = \int_0^\theta \frac{F_{01}(\theta) + F''_{01}(\theta)}{\sqrt{3}\, F_{01}(\theta)}\, d\theta. \tag{30}$$

Note that the equivalent strain is independent of r, and hence the shear stress must be.

The equilibrium equations now only involve the variation of the mean normal stress, σ, and the angular variation of the shear stress:

$$\frac{1}{r}\frac{\partial \sigma_{r\theta}}{\partial \theta} + \frac{\partial \sigma}{\partial r} = 0,$$
$$\frac{1}{r}\frac{\partial \sigma}{\partial \theta} + \frac{2\sigma_{r\theta}}{r} = 0. \tag{31}$$

Cross–differentiating to eliminate σ:

$$\frac{\partial^2 \sigma}{\partial r \partial \theta} = -\frac{1}{r}\frac{\partial^2 \sigma_{r\theta}}{\partial \theta^2} = -2\frac{\partial \sigma_{r\theta}}{\partial r} = 0,$$

since $\sigma_{r\theta} \neq f(r)$.

Thus there is only a linear dependence of stress on θ:

$$\frac{d\sigma_{r\theta}}{d\theta} = \frac{d\sigma_{r\theta}}{d\gamma_{r\theta}}\,(\gamma_{r\theta}) \cdot \frac{d\gamma_{r\theta}}{d\theta} = C,$$

or

$$\frac{d\sigma_{r\theta}}{d\gamma_{r\theta}}\left(\int_0^{\theta}\left[1+\frac{F''_{01}(\theta)}{F_{01}(\theta)}\right]d\theta\right)\cdot\left[1+\frac{F''_{01}(\theta)}{F_{01}(\theta)}\right] = C. \tag{32}$$

It thus appears that strain hardening materials can develop a sharp crack with rigid–body motion approaching and leaving the crack region. Even more possibilities exist in the presence of deformation in front of the crack. These possibilities require knowledge of the boundary conditions at large r. Further investigation is beyond the scope of this paper, and we turn to non–hardening solutions for which the complete flow fields are known.

4. For *non–hardening plastic flow in a symmetrical, doubly grooved specimen* the field is shown in Fig. 12. Following Neimark[10], the velocities in the fan relative to the center of the

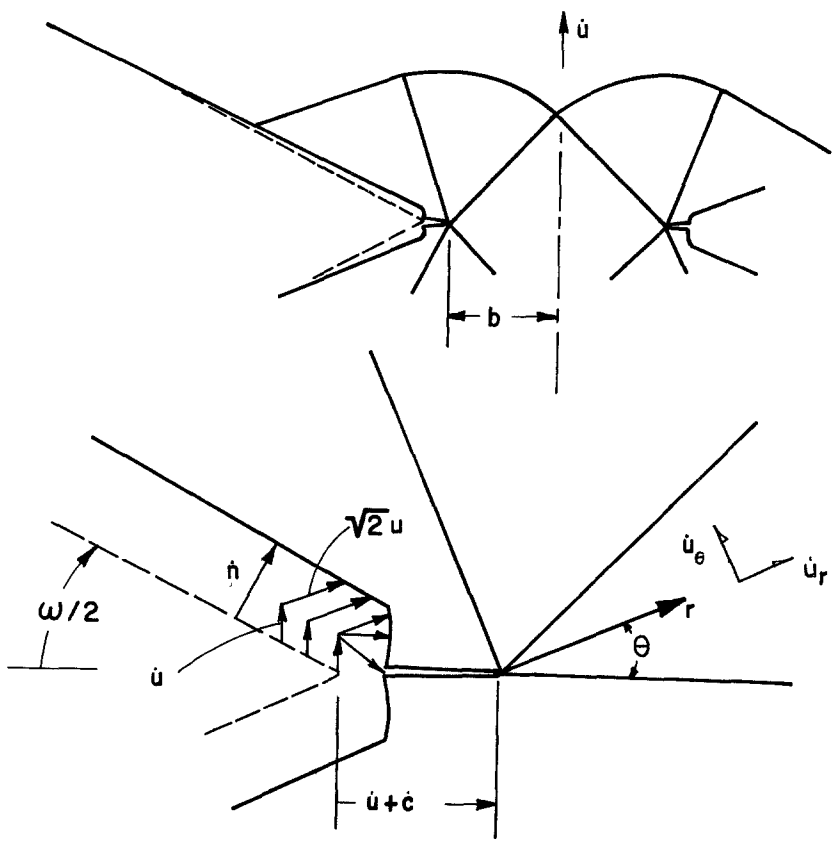

Fig. 12. General and detailed views of steady–state cracking and displacements in a doubly grooved tensile specimen.

specimen are found by adding the simple ones, viewed relative to the upper rigid region, to the velocity of that region relative to the center:

$$\dot{u}_r = 0 + \dot{u}\sin\theta,$$

$$\dot{u}_\theta = -\dot{u}(\sqrt{2}-r/b) + \dot{u}\cos\theta. \tag{33}$$

By itself, this velocity field would cause the flank at the crack tip to be displaced normally at the rate

$$\dot{n} = \frac{1}{\sqrt{2}}(\dot{u}_r - \dot{u}_\theta)_{\theta=\frac{3\pi}{4}-\frac{\omega}{2}} = \dot{u}(1 + \cos\omega/2), \tag{34}$$

shown in Fig. 12, while the root advances by

$$\dot{x}_{root} = \dot{u}. \tag{35}$$

Thus blunting occurs unless there is simultaneous crack growth $\dot{c}$, giving the angle

$$\sin\omega/2 = \frac{\dot{n}}{\dot{u}+\dot{c}} = \frac{\dot{u}}{\dot{u}+\dot{c}}(1 + \cos\omega/2), \quad \text{or} \quad \frac{\dot{u}}{\dot{u}+\dot{c}} = \tan\omega/4. \tag{36}$$

The factor $\dot{u}/(\dot{u}+\dot{c})$, which may be called the crack propagation ductility (CPD), ranges from 0 to 1 as $\dot{c}/\dot{u}$ ranges from ∞ to 0. The included angle ω observed during crack propagation may therefore provide a useful index of ductility.

Now take the velocities in the fan relative to the crack tip, so that Eqs. 33 become

$$\begin{aligned} \dot{u}_r &= \dot{u}\sin\theta - (\dot{c}+\dot{u})\cos\theta, \\ \dot{u}_\theta &= \dot{u}\cos\theta - \dot{u}(\sqrt{2} - \frac{r}{b}) + (\dot{c}+\dot{u})\sin\theta. \end{aligned} \tag{37}$$

For comparison with the general formulation the stream function is

$$\begin{aligned} \psi &= rF_{01}(\theta) + r^2F_{02}(\theta) \\ &= -r\dot{u}\left[\cos\theta + \left(\frac{\dot{c}+\dot{u}}{\dot{u}}\right)\sin\theta - \sqrt{2}\right] - \frac{r^2\dot{u}}{2b}. \end{aligned} \tag{38}$$

The strain rates are

$$\begin{aligned} \dot{\epsilon}_r &= 0 = -\dot{\epsilon}_\theta, \\ \dot{\gamma}_{r\theta} &= \sqrt{2}\dot{u}/r. \end{aligned} \tag{39}$$

The rotation that is important in hole growth is the rotation of the material element relative to that of the stress field. The rotation of the element is

$$\dot{\phi} = \frac{1}{2}\left(\frac{\partial\dot{u}_\theta}{\partial r} + \frac{\dot{u}_\theta}{r} - \frac{1}{r}\frac{\partial\dot{u}_r}{\partial\theta}\right) = \frac{\dot{u}}{b} - \frac{\dot{u}}{\sqrt{2}r}, \tag{40}$$

while that of the stress field in the fan is

$$\dot{\phi}_{stress} = -\frac{\dot{u}\sqrt{2}}{r} + \frac{\dot{u}}{b} + \frac{\dot{u}\cos\theta}{r} + \frac{(\dot{c}+\dot{u})\sin\theta}{r}, \tag{41}$$

giving a relative rotation of

$$\dot{\phi}_{rel} = \frac{\dot{u}}{\sqrt{2}r} - \frac{\dot{u}\cos\theta}{r} - \frac{(\dot{c}+\dot{u})\sin\theta}{r}. \tag{42}$$

With $(\dot{u} + \dot{c})/\dot{u}$ from Eq. 36, the rotation is opposite in sign to that of the shear strain (Eq. 39), whereas the shear band analysis (Eqs. 9 through 11) was for rotation and shear with the same sign. The effect here is to open up the holes, and the damage rate will probably be greater. Nonetheless, for illustrative purposes we take the damage rate to follow the same Eqs. 9 through 11. While the damage rate could in principle be integrated through the fan, if the fracture criterion were not satisfied until near the trailing edge of the fan, the resulting crack would tend to blunt the main crack and no steady state propagation would occur. Such lateral fractures are frequently observed, and, in fact, it is difficult to run tests on high strength aluminum alloys without encountering them. If, on the other hand, fracture occurs soon after an element enters the fan, the crack progresses at 45° and the chances of zig–zagging, macroscopically normal fracture are much increased. We therefore estimate the initial damage rate per unit angle traversed.

The damage rate, based on mean radius growth alone for further simplicity, may be defined in terms of the variables of Eq. 11 as

$$\frac{\partial \eta}{\partial \gamma} \equiv \frac{1}{\ell n\, L/2R_1} \frac{\partial\, \ell n\, R/R_1}{\partial \gamma}. \tag{43}$$

The mean normal stress is related to the included crack angle and the yield strength in shear $\tau = k$ by

$$\sigma = k(1 + \pi - \omega). \tag{44}$$

The shear strain per unit angular travel at $\theta = 45°$, $r \ll a$ turns out to be

$$\frac{d\gamma}{d\theta} = \frac{\dot{\gamma}_r}{\dot{u}_\theta} = \frac{2u}{\dot{c}} = \frac{2}{\cot \frac{\omega}{q} - 1}. \tag{45}$$

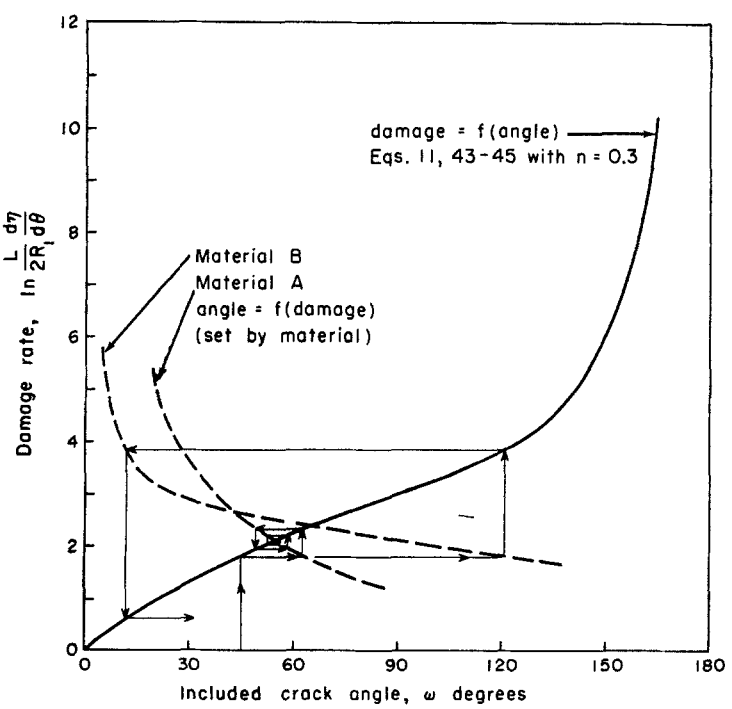

Fig. 13. Stability of steady–state crack growth in doubly grooved, plane strain tension. (Total strain in fan approaches 2 as $\theta \to 180°$).

Combining Eqs. 11 and 43 through 45, along with the assumption that n = 0.3, allows calculation of the damage rate, shown in Fig. 13.

Suppose now that the fracture process sets some relation between damage rate and crack propagation ductility, or, through Eq. 36, the included crack angle. Two such possible relations are sketched in Fig. 13 as dashed lines. The intersection of these lines, giving material response to a given damage rate, with 'geometrical' lines, giving the damage rate for a given included angle, sets the steady state angle.

The question of stability is important. Assume, as indicated in Fig. 13, that the initial notch angle is about 45°. The corresponding damage rate is about 1.8. For Material B, the resulting crack angle will be 120°. As this develops, the 'geometry' (including the effect of the strain hardening coefficient n in Eq. 43) gives a damage rate of about 3.8. Continuing around the loop indicates that the process blunts the crack completely. With Material A, the process is convergent. The question of stability is not so much one of ductility, as of the relative slopes of the curves. The condition for steady state crack growth seems to be

$$\left[\frac{d(d\eta/d\theta)}{d\omega}\right]_{\text{'geometry'}} \left[-\frac{d\omega}{d(d\eta/d\theta)}\right]_{\text{material}} < 1. \tag{46}$$

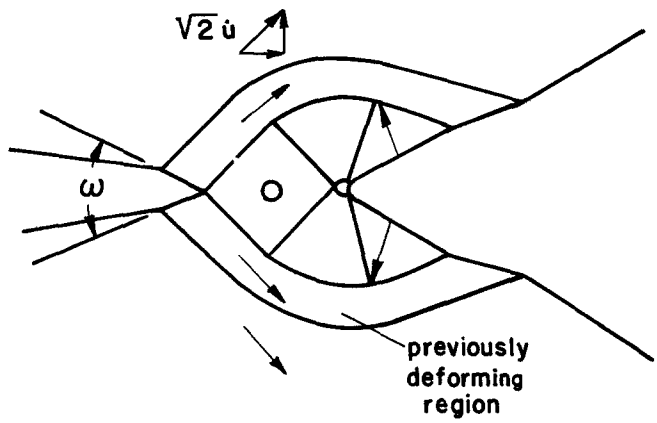

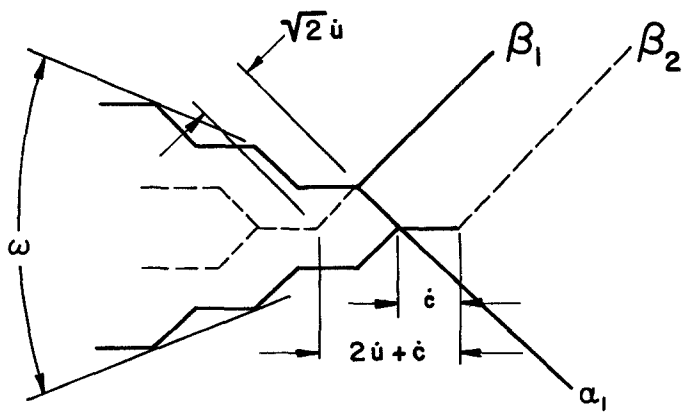

Fig. 14. General and detailed views of steady–state cracking and displacements relative to core in asymmetric plane strain tensile specimen.

Actually, of course, these paths will not be strictly followed because transient changes in the crack angles will cause corresponding changes in the damage rates even before steady state is reached. Likewise, the steady state condition is probably only approximate.

5. For the growing crack in an *asymmetrically grooved tensile specimen,* shown in Fig. 14, the opening occurs under alternating slip by $\sqrt{2}\dot{u}$ along the slip lines α, β at $\theta = \pm 45°$, with a cracking $\dot{c}$ superimposed. The crack opening angle ω is related to the crack propagation ductility (CPD) in a different way than for the doubly grooved case, Eq. 36:

$$\tan \omega/2 = \frac{\dot{u}}{\dot{u} + \dot{c}} = \text{CPD}. \tag{47}$$

The discontinuity in $\dot{u}_r$ makes it easier to find the shear strain directly rather than through the displacement function, Eqs. 24 through 26. The average shear strain between each pair of slip lines is

$$\gamma = \frac{\sqrt{2}\dot{u}}{(2\dot{u} + \dot{c})/\sqrt{2}} = \frac{2}{1 + 1/(\text{CPD})} = \frac{2}{1 + \cot \omega/2}, \tag{48}$$

which varies from 0 to 1 as the crack propagation ductility goes from 0 to 1 (or the included angle ω from 0 to $\pi/2$).

6. *Single Slip* can be produced by unequal, asymmetric grooves, as discussed by Green[47] and mentioned in Par. A2 of the section here on crack initiation. The resulting slip is shear on a single plane, as in circumferentially grooved torsion, but with a stress that is combined Mode I and II.

7. *Discussion of fully plastic solutions.*

a) The fan and slip band fields considered here for pure tension are also found around growing cracks under bending, (the variation of velocities with θ will be somewhat different, but not significantly so if only the initial strain rate in the fan is considered).

b) One of the surprising features of the non–strainhardening, plane strain, tensile (Mode I) solutions is the disappearance of any dependence of strain on radius, in contrast to torsion of a longitudinal groove. This seems to arise from the result that there is either no strain, or uniform strain, in the region directly in front of the crack. The absence of a dependence on radius means that for these geometries it is dimensionally impossible to obtain k_{1c} data from fully plastic tests, in contrast to torsion of longitudinal grooves, where such data can be obtained.

c) The absence of strain directly in front of the crack also makes it likely that often rather than pure Mode I fracture, a macroscopically normal fracture consists of alternating combined Mode I and Mode II fracture as observed for example by Bluhm and Morrissey[48] and Alpa'igh[13]. The rotation of active slip lines through the material may provide a dependence of strain on radius, although space and time do not permit an analysis here.

C. Modes of Propagation

1. *Cleavage* is the classical mode of crack propagation, and occurs by the separation of a single plane, as discussed in some detail by Barenblatt and Broberg at this conference, for example. Griffith was able to use an energy argument because, in effect, the elastic calculations for the body which Griffith used described all of the medium except a thin layer in the path of the crack. The work done on this thin layer is the surface energy, and comes from the energy drained out of the surrounding elastic region. The reversibility in both the linear elastic region and the surface layer mean that detailed calculations of the fracture process are not required.

Where plastic deformation is confined to a single line, so that the loading is radial (constant

ratios of the principal stress) and where any residual stresses are eliminated from the material by the advancing crack, and where the forces across the line are known from some fracture criterion, the energy balance still affords a solution.

For compression, Griffith had to abandon the energy point of view because energy release rates were not (and still are not) available for the z–shaped cracks which develop. Also, where a plastic zone extends out of the plane of the crack, the energy point of view becomes of little help because calculation of the elastic energy in the form of residual stress and the plastic work left behind by the growing cracks requires a detailed study of the flow processes in the plastic region, as well as an appropriate fracture criterion, based on the actual metallurgical processes involved, as discussed in this paper.

2. *Dislocation nucleation in a perfect crystal* may be preferred to cleavage. The choice between these alternatives has been studied in a preliminary way by Kelly et al.[49] Here it is necessary to consider the atomic configurations to either side of the crack as well as directly in front of it.

3. *Twinning and de–twinning,* suggested by Suzuki[50] for iron, is in effect a combination of the first two mechanisms in which the dislocations drop back into the crack along its flank, returning the crystal lattice to its original shape and leaving a sharp crack even in the presence of plastic deformation. This is an interesting speculation which is difficult to check either theoretically or experimentally.

4. *Plane strain rupture* might be regarded as a macroscopic example of the twinning mechanism mentioned by Suzuki. It could conceivably occur in materials with a high enough plastic strain. The size effect in fracture would have to arise from the dimensions of the Burgers vector or the dislocation spacing.

5. *Plane stress fracture* has been observed in a variety of foils and therefore provides one case in which products can separate purely as a result of mechanics without any fracture criterion at all. The size dimension is provided by the thickness of the foil or sheet.

6. *Sliding off* occurs on many fracture surfaces, as for example, those around the inclusion in Fig. 8 or near the tip of very sharp notches. This does not represent metallographic mode of fracture, but simply what has been called serpentine glide by Beacham. This is apparently micro or macroscopic evidence for the alternate shearing either side of a crack tip which can lead to the opening of a 90° notch. In most cases the plastic deformation arises from dislocations in the material around the notch tip breaking through to the notch, rather than from nucleation of dislocations at the notch tip.

7. *Repeated nucleation* to propagate cracks occurs in addition to those mechanisms of crack growth discussed above, which are unique to crack propagation. Re–nucleation has frequently been observed in the cleavage crack propagation in iron and no doubt gives rise to the parabolic fracture markings in ductile fracture. As pointed out by McClintock[51] this process very likely occurs very close to the crack tip and the interaction of the growing holes and cracks must be considered.

A specific example of re–nucleation of fracture by hole growth ahead of the notch has recently been analyzed by studying the possibility of hole growth in the blunted region ahead of the growing crack (McClintock[52]). It was assumed that when the fracture criterion was satisfied at some point within the logarithmic spiral region growing ahead from a blunting notch, fracture would immediately occur from the current crack tip to the point at which the fracture criterion was satisfied. The sharp notch thus produced would again blunt until a logarithmic spiral region swept over another fracture site, and so on.

In this blunting mechanism the distance into the spiral at which fracture nucleates is the

analogue of the angular distance into the fan at which fracture occurs in the more macroscopic point of view which neglects details at the crack tip.

The following conclusions were reached for fracture by repeated re–nucleation of holes in a blunting groove.

i. The blunting of cracks provides a strain concentration directly in front of the crack that is greater than that on either flank. This concentration, which is absent with sharp cracks, can lead to continued crack growth in the original direction.

ii. Analysis of the strain distribution in front of the growing crack indicates that for steady state propagation only one fracture nucleus at a time is within the logarithmic spiral region. Specimens of total thickness equal to 1000 times the nucleus spacing are required to produce quasi–steady state fracture due to strain in the spiral region, in preference to fracture nucleation in the core.

iii. Aside from the specimen size required to regard the shape of the specimen in a continuous manner, there is no dependence of fracture strain or crack propagation rate on the initial spacing of the fracture nuclei. Thus it is dimensionally impossible to determine the stress singularity factor K_{1c} from tests on these specimens. This is in contrast to torsion of longitudinally grooved bars, where K_{3c} can in principle be determined from fully plastic torsion.

iv. High strain concentrations in front of the crack caused by shear to either side would appear to support the proposal by Wells that the displacements between the flanks of the crack should correlate fracture because much (although not all) of this displacement contributes to the strain distribution in front of the crack. As mentioned in conclusion iii, however, the analysis fails to bear out the correlation.

v. In ductile fracture by the growth of holes, the growth of the hole will react strongly with the blunting of the crack. Probably the two effects must be considered simultaneously.

vi. Where relatively brittle fracture requires high triaxiality but very low plastic strain, fractures may be repeatedly nucleated at the tip of the logarithmic spiral region.

vii. The sharp cracks observed in elastic–plastic fracture probably depend on reversed plastic flow and require a separate analysis.

Experiments on OFHC copper to check the analysis showed that fracture initially occurred by sliding off in a sharp 90° notch followed by a shear fracture arising from hole growth along two 45° planes running upward from either notch. In 1100 aluminum it was frequently observed that the sharp notches became flat–bottomed rather than round. A reexamination of the analysis by Wang[15] on which the fracture study was based, indicates that plasticity theory may well suggest flat–bottomed notches rather than sharp ones. In aluminum the flat–bottomed configuration was unstable, with one of the corners growing ahead of the others and forming a new crack. Sometimes cracks grew from both sharp corners. When one became dominant, a flake of aluminum was left attached to the other surface. Space and time prevent further discussion of these results.

With a sufficiently high ratio of crack advance to normal displacement, the angle of the steady state crack growth may be so small, say of the order of the yield strain, that it may be embedded in an elastic stress field. Such fine cracks have been observed by Bluhm and Morrissey[48], Alpaugh[13], Henry[53] and others in the fracture of tensile specimens, where, although initially plastic the final crack propagation in high strength materials seems to be caused by the compliance of the material in the neck of the specimen. Henry[53] has developed an approximate solution based on an analogy with the Mode III distribution of stress and strain in the similar case.

CONCLUSIONS

1. Many kinds of criteria are needed for the different stages of the nucleation and growth of cracks. Sometimes one of these stages provides an explanation on a finer scale of what at a larger scale of observation appears to be a single process. Other times the fracture occurs by the simultaneous operation of several mechanisms of failure rather than by their sequential operation.

2. It begins to appear that a true Mode I fracture may be rare in ductile fracture. Rather the fracture process consists of combined Modes I and II or combined Modes I and III.

3. Because of the wide variety of materials and conditions of fracture it is safe to conclude that nearly every self consistent theory is right for some conditions in some material.

4. In order to obtain a more quantitative understanding of ductile fracture there is a desperate need for more plasticity solutions. Even so, solutions are presented for steady state growth of cracks in plane–strain deformation of a non–strainhardening material in tension and torsion.

5. The possibility of simultaneous diffuse and concentrated (Dugdale–Muskhelishvili) flow fields is demonstrated for torsion of longitudinally grooved bars.

Acknowledgement. The author wishes to thank Regis M.N. Pelloux for the micrographs in Figs. 8 and 9, Helmut Huff for the analysis of non–hardening plastic flow past cracks as well as the corresponding experiments, and James H. Williams, Jr. for Figs. 2 and 3. James H. Williams, Jr.

ACKNOWLEDGEMENTS

The author wishes to thank Regis M.N. Pelloux for the micrographs in Figs. 8 and 9, Helmut Huff for the analysis of non–hardening plastic flow past cracks as well as the corresponding experiments, and James H. Williams, Jr. for Figs. 2 and 3, James H. Williams, Jr. and Robert Hodges contributed to the design of specimens for studying the effect of triaxiality on fracture initiation. The financial support of the Massachusetts Institute of Technology and of the National Science Foundation is greatly appreciated. Finally the author is deeply indebted to the Swedish National Committee for Applied Mechanics, in particular Folke K.G. Odqvist and Janne Carlsson, for focussing attention on the need for fracture criteria in front of a growing crack, and for the conference at which it became clear that the diffuse and concentrated plastic flow fields might not only each be appropriate in different cases, but might also coexist.

Received November 27, 1967.

REFERENCES

1. J.R. Rice — *J. Appl. Mech. 34*, 287–298, (1967).

2. A.A. Griffith — *Proc. First Inter. Cong. Appl. Mech. (Delft)*, 55–63, (1924).

3. E. Orowan — *Rpt. Prog. Phys. 12*, 185–232, (1949).

4. F.A. McClintock — *J. Appl. Mech. 35*, 363–371, (1968).

5. C.A. Berg — *Proc. 4th U.S. Nat. Cong. Appl. Mech. 2*, 885–892, (1962).

6. R. Hill — *The Mathematical Theory of Plasticity*, Oxford University Press, (1950).

7. W. Prager, P.G. Hodge, Jr. — *Theory of Perfectly Plastic Solids*, John Wiley & Sons, Inc., New York, (1951).

8. F.A. McClintock — *Welding J. Res. Suppl. 26*, 202–208, (1961).

9. B.B. Hundy — *Metallurgia 49*, 109–118, (1954).

10. J.E. Neimark — *J. Appl. Mech. 35*, 111–116, (1968). For shoulder width, see also D.J.F. Ewing and R. Hill, *J. Mech. Phys. Solids 15*, 115–124, (1967).

11. R. Hill — *J. of Mech. Phys. Solids, 6*, 236–249. See also *J. of Mech. Phys. Solids, 5*, 302–307, (1958).

12. B.I. Edelson, W.M. Baldwin, Jr. — *Trans. Quart. A.S.M. 55*, 230–250, (1962).

13. H.E. Alpaugh, Jr. — 'Investigation of the Mechanisms of Failure in the Ductile Fracture of Mild Steel', B.S. Thesis, Dept. of Mech. Eng., M.I.T., Cambridge, (1965).

14. R. Hodges — 'An Experimental Study of Crack Growth Instability in Fully Plastic Tensile Specimens', B.S. Thesis, Dept. of Mech. Eng., M.I.T., Cambridge, (1967).

15. A.J. Wang — *Quart. Appl. Math. 11*, 427–438, (1954).

16. W.N. Findley, D.C. Drucker; D.J.F. Ewing, R. Hill — *J. Appl. Mech. 32*, 493–503, (1965); *J. Mech. Phys. Solids, 15*, 115–124 (1967).

17. A. Guillen–Preckler, F.A. McClintock, R.D. White — *Proc. 1st Int. Conf. Fracture, Sendai 1*, 411–427, (1966).

18. P.W. Bridgman — *'Studies in Large Plastic Flow and Fracture'*, McGraw Hill, New York, (1952).

19. D.P. Clausing — 'The Tensile Fracture of Mild Steel', PhD. Thesis, Calif. Inst. of Tech., Pasadena, (1966).

20. K.C. Norris — 'Strain in the Neck of a Tensile Specimen', M.S. Thesis, M.I.T., Dept. of Mech. Eng., Cambridge, (1967).

21. F.A. McClintock — *Materials Res. and Standards, 1*, 277–279, (1961).

22. A.R. Rosenfield, P.K. Dai, G.T. Hahn — *Proc. First Int. Conf. on Fracture, Sendai 1*, 223–258, (1966).

23. J.L. Swedlow, M.L. Williams, W.H. Yang — *Proc. 1st Int. Conf. Fracture, Sendai 1*, 259–282, (1966).

24. D.A. Bateman, F.J. Bradshaw, D.P. Rooke — 'Some Observations on Surface Deformation Round Cracks in Stressed Sheets', R.A.E. Tech. Note CPM 63, Ministry of Aviation, London W.C. 2, (1964).

25. J.B. Walsh, A.C. Mackenzie — *J. Mech. Phys. Solids 1*, 247–257, (1959).

26. I. Kayan — 'Crack Initiation and Crack Growth Process on Rectangular Cross Sectional and Longitudinally Notched Bars Under Plastic Torsion', Research Memo 17, Fatigue and Plasticity Lab., M.I.T., Dept. of Mech. Eng., (See also: R.D. Landis, 1962, 'Crack Initiation in Rectangular Longitudinally Grooved Specimens Under Plastic Torsion II', Research Memo 37, Fatigue and Plasticity Lab., M.I.T., Dept. of Mech. Eng., Cambridge, (1959).

27. F.A. McClintock, W.R. O'Day, Jr. — *Proc. 1st Int. Conf. Fracture, Sendai 1*, 75–98, (1965).

28. C.P. Sullivan — *Welding Research Council Bulletin 122*, New York, (1967).

29. J.J. Gilman — *J. Metals 6*, 621–629, (1954).

30. A.N. Stroh, — *Phil. Mag. 3*, 597–606, (1958).

31. A. Deruyttere, G.B. Greenough — *J. Inst. Met. 84*, 337–345, (1956).

32. T.L. Johnston, R.J. Stokes, C.H. Li — *Phil. Mag. 7*, 23–24, (1962).

33. D. Hull	*Acta Met. 8*, 11–18, (1960).
34. A.H. Cottrell	*Fracture*, B.L. Averbach et al., eds., Wiley, New York, 20–53, (1959).
35. R.J. Brinkerhoff	'Elastic–Plastic Strain Fields for a Cylindrical Inclusion in Shear', M.S. Thesis, Dept. of Mech. Eng., M.I.T., Cambridge, (1966). See also (41).
36. A. Kelly, G.J. Davies	*Metallurgical Reviews 10*, 1–78, (1965).
37. I.G. Palmer, G.C. Smith	*2nd Bolton Landing Conf. on Oxide Dispersion Strengthening*, Lake George, New York (1966).
38. V.A. Tipnis, N.H. Cook	*J. Basic Eng. Trans. ASME 89D*, 533–540, (1967).
39. J.F. Knott, A.H. Cottrell	*J. Iron and Steel Inst. 201*, 249–260, (1963).
40. F.A. McClintock, S.M. Kaplan, C.A. Berg, Jr.	*Int. J. Fracture Mech. 2*, 614–627, (1966).
41. F.A. McClintock	'On the Mechanics of Fracture from Inclusions', ASM Seminar on Ductility, Cleveland Ohio, (1967).
42. P.J.E. Forsyth, C.A. Stubbington, R.N. Wilson	'The Growth of Free Slip Paths as a Primary Cause of Fatigue in Metals', RAE Tech. Note Met–Phys. 333, Ministry of Aviation, London W.C. 2, (1961).
43. F.A. McClintock	Discussion *in Fatigue in Aircraft Structures* A.M. Freudenthal, Ed., Academic Press, New York, 78–79, (1956).
44. F.A. McClintock, A.S. Argon, editors	*Mechanical Behavior of Materials*, Addison Wesley, Reading, Mass., 522, (1966).
45. F.A. McClintock	*Proc. Int. Conf. Fatigue of Metals, Inst. Mech. Eng.*, 538–542, (1956).
46. H.C. Rogers,	*Trans. Met. Soc. AIME 218*, 498–506, (1960).
47. A.P. Green	*J. Mech. Phys. Solids 2*, 197–211, (1954).
48. J.I. Bluhm, R.J. Morrissey	*Proc. 1st Int. Conf. Fracture, Sendai 3*, 1739–1780, (1966).
49. A. Kelly, W.R. Tyson, A.H. Cottrell	*Phil. Mag. 15*, 567–586, (1967).
50. H. Suzuki	*Proc. 1st Int. Conf. Fracture, Sendai 2*, 613–614, (1966).
51. F.A. McClintock	*Proc. Roy. Soc. A 285*, 58–72, (1965).
52. F.A. McClintock	'Crack Growth in Fully Plastic Grooved Tensile Specimens', Research Memo 105, Fatigue and Plasticity Lab., M.I.T., Dept. of Mech. Eng., Cambridge, (1966); *Physics of Strength and Plasticity*, MIT Press, (1969).
53. M.F. Henry	'An Investigation of Fine Cracks in Ductile Fracture , M.S. Thesis, Dept. of Mech. Eng., M.I.T., Cambridge, (1966).

RÉSUMÉ – On passe en revue les distributions de déformations dans les éprouvettes susceptibles de permettre d'étude de l'amorçage de la rupture, et l'on met l'accent sur les configurations relatives à la propagation statique de fissures amorcées dans des matériaux entièrement plastiques sollicités en état de déformation.

Les diverses formulations mathématiques des critères de rupture locale sont discutées en fonction de différents types de mécanismes métallurgiques. On conclut de cette étude que:

1° Hormis les cas où se rencontre le clivage, une rupture de mode 1 (normale) a peu de chances de survenir.

2° Le développement de fissures aigues et de fissures à fond plat est mis en évidence à la fois sur le plan théorique et sur le plan expérimental.

3° Dans des barres nanties d'une rainure longitudinale et soumises à torsion il peut survenir simultanément des champs découlement plastique sans frontières bien précises et de type concentré (Dugdale–Muskhelishvili) lorsque la courbe tension dilatation présente un maximum qui, en provoquant la formation d'une bande de glissement, rend approprié le recours à un critère de déplacement pour justifier la rupture finale.

ZUSAMMENFASSUNG – Es wurden Spannungsverteilung an Proben, die zum Studium für die Entstehung von Brüchen geeignet sind, nachgeprüft. Verteilungen für die Fortpflanzung der Risse im Festzustand bei planarer Anspannung und mit völlig plastischem Material, wurden entwickelt. Das funktionelle Verhalten von örtlichen Bruchmerkmalen für verschiedene metallurgische Mekanismen wurde diskutiert. Folgendes wurde festgestellt:

a) es ist unwahrscheinlich, dass ein exclusiver Modus I (normal) Bruch besteht, ausser bei Teilung.

b) es besteht theoretischer und experimenteller Beweis für die Entwicklung von spitzflächigen und flachbödigen Rissen.

c) gleichmässig weitverbreitete und konzentrierte (Dugdale–Muskhelisvili) Flussfelder können in Drehungen von länglich gerillten Riemen vorkommen, wenn die Beanspruchungskurve ein Maximum hat, das Riemenbildung verursacht, so dass ein Verformungsmerkmal für den Endbruch zweckmässig wird.